

The following publication Rinaldi, L., Yeung, L. F., Lam, P. C. H., Pang, M. Y., Tong, R. K. Y., & Cheung, V. C. (2020). Adapting to the Mechanical Properties and Active Force of an Exoskeleton by Altering Muscle Synergies in Chronic Stroke Survivors. *IEEE Transactions on Neural Systems and Rehabilitation Engineering*, 28(10), 2203-2213, is available at <https://dx.doi.org/10.1109/TNSRE.2020.3017128>.

## Normalization of Lower-Limb Muscle Synergies during Gait Training with a Powered Ankle Exoskeleton in Chronic Stroke Survivors

Linda Rinaldi<sup>1</sup>, Ling-Fung Yeung<sup>2</sup>, Patrick Lam<sup>1</sup>, Marco Pang<sup>3</sup>, Raymond Kai-Yu Tong<sup>2</sup>, Vincent C. K. Cheung<sup>1,4#</sup>

<sup>1</sup> School of Biomedical Sciences, and The Gerald Choa Neuroscience Centre, The Chinese University of Hong Kong, Hong Kong, China

<sup>2</sup> Department of Biomedical Engineering, The Chinese University of Hong Kong, Hong Kong, China

<sup>3</sup> Department of Rehabilitation Sciences, The Hong Kong Polytechnic University, Hong Kong, China

<sup>4</sup> The KIZ-CUHK Joint Laboratory of Bioresources and Molecular Research of Common Diseases, The Chinese University of Hong Kong, Hong Kong, China

# Corresponding author

**Abstract.** Chronic stroke survivors often suffer from debilitating gait impairment resistant to intervention. Recent rehabilitation strategies based on gait training with powered exoskeleton appear promising, but whether chronic survivors may benefit from them remains controversial. We seek to evaluate, in chronic survivors, the potential of exoskeletal gait training in reducing impairment by restoring the normal muscle activation patterns underpinned by normal muscle synergies. The exoskeleton tested was a unilateral ankle-foot orthosis that produced modulated assistive torque. Over a single session, chronic survivors (N = 10) walked over-ground without exoskeleton, then with exoskeleton turned off and then on, while electromyographic signals (EMGs, 28 muscles both sides) were recorded. Muscle synergies were identified from EMGs using non-negative matrix factorization. Gait with exoskeleton, off or on, resulted in alterations of paretic-side muscle synergies and their temporal activations. Gait with the assistive force turned on further increased the similarity between the synergies of the paretic and non-paretic sides, but this similarity increase was dependent on the subjects' residual motor status as indicated by clinical scores. Our results argue that powered exoskeleton could elicit, over a single session, closer-to-normal muscle synergies in some chronic survivors, thus supporting its potential use as a rehabilitation that drives neuroplasticity towards the direction of true recovery from impairment.

## INTRODUCTION

In humans, stable, coordinated and yet flexible gait is achieved when the central nervous system (CNS) recruits specific groups of muscles that are activated as individual units called muscle synergies. A cerebrovascular accident (CVA) in the CNS that lasts only for a few minutes may impair motor abilities by damaging the neuronal networks that activate or encode these locomotor muscle synergies. As a result of reduced muscle strength and disrupted proprioception and motor coordination, stroke survivors often face permanent motor impairment (Murray et al. 2015), including asymmetric gait with abnormal ranges of motion for multiple joints, foot drop, reduced walking speed, and co-contraction of agonist and antagonist muscles on the stroke-affected leg (Hashiguchi et al. 2016, Safavynia et al. 2011, Pennycott et al. 2012). Such reduced gait performance is likely related to changes in the muscle synergies and their patterns of activation on the stroke-affected side after the CVA (Cheung et al. 2012, Hashiguchi et al., 2016, Safavynia et al. 2011, Allen et al., 2013, Clark et al. 2010, Gizzi et al. 2011).

Chronic stroke survivors with locomotor impairment may functionally benefit from gait retraining. Even though recent studies have demonstrated that some degree of motor recovery is possible for very chronic stroke survivors (Teasell et al. 2014), in general current rehabilitation strategies only produce modest motor gains that are mostly achieved within the first 6 months after the CVA (Meyer et al. 2016, Pennycott et al. 2012). For chronic survivors participating in rehabilitation programs, there is considerable uncertainty in the outcome of the rehabilitation given the current lack of knowledge of how exactly each survivor should be best trained for maximal motor gain. As a consequence, rehab protocols for chronic survivors are generally based on standard physiotherapy combined with cardio training or exercises for strengthening muscles (Dickstein 2008, Polese et al. 2013, Mehta et al. 2012, Winstein et al. 2016, Lamola 2014). Development of new interventional strategies for chronic stroke survivors that consistently result in recovery beyond that achievable with standard interventions are critically needed.

Among the various new gait rehabilitation strategies, those based on motor training on powered exoskeletons are currently considered to be some of the most promising for maximizing motor gain, especially for sub-acute stroke survivors (Bortole et al. 2015, Kasai et al. 2015, Miljkovi et al. 2013, Louie and Eng, 2016). Exoskeletons are robotic interactive wearable devices designed to actively assist motor-impaired subjects during overground walking by sensing their walking intention, and consequently adjusting their abnormal gait patterns by providing suitable assistive forces to the stroke-affected leg (Yeung et al. 2017). A large-scale evaluation of the clinical benefits associated with gait training on exoskeletons is currently underway, but numerous smaller trials have argued for their effectiveness in improving gait for some, but not all, chronic survivors (Louie and Eng, 2016). Precisely how rehabilitative exoskeletons should be designed and utilized for providing personalized motor training that maximizes motor recovery for diverse stroke survivors has remained an open question that urgently demands an answer.

Here, we argue that understanding the neural mechanisms underlying any motor recovery induced by human-exoskeleton interactions should help unleash the full rehabilitative potential of exoskeletons. Such an understanding should also facilitate the eventual development of

rehabilitative or prosthetic devices that respond directly to CNS commands delivered through a neural interface on the wearable (Pons, 2019). Currently, this understanding is lacking due to the enormous complexity of both locomotor control and the neuroplastic processes involved over different stages of rehabilitation (Alia et al. 2017, Sylos-Labini et al. 2014). One way to begin dissecting such neural mechanisms is to characterize the changes in the muscle activation patterns induced by exoskeletal training. The organization of the multi-muscle patterns can be clarified with a muscle synergy analysis (Safavynia et al. 2011, Cheung et al. 2019) that decomposes the experimental muscle patterns into a small number of time-invariant muscle synergies, usually by a factorization algorithm. Indeed, the neural basis of factorization-derived muscle synergies has been demonstrated (Takei et al. 2017). Thus, different from clinical assessments, muscle synergy analysis may shed light on the *precise* effects exerted by exoskeletal training on the stroke-impaired motor system, and allow us to evaluate whether the training protocol is able to induce a reorganization of the disrupted motor patterns towards the normal patterns utilized before stroke for gait.

At present, very few powered lower-limb exoskeletons have been evaluated on stroke survivors from a muscle-synergy perspective. In particular, their effects on muscle synergies have been mostly explored either in neurologically intact individuals or acute stroke survivors (Gizzi et al. 2012, Steele et al. 2018, Jacobs et al. 2018). In acute survivors, preliminary results have suggested that exoskeletal training may improve motor outcome by increasing the inter-leg similarity of the muscle synergies (Tan et al., 2018).

The present work aims to investigate the within-session effects induced by an exoskeleton-based gait training on the lower-limb muscle synergies in motor-impaired chronic stroke survivors. Considering that the degree of motor recovery beyond 3 months post-stroke is normally much smaller than that within the first weeks after stroke (Semrau et al. 2015), it would be important to understand if robotic exoskeletal training could reduce motor impairment even in the chronic phase. To address our question, we selected a robotic ankle foot orthosis (AFO) with features including light weight, untethered power supply system, and unilateral design for easy portability during overground walking. Specifically, we ask whether chronic stroke survivors could walk with the AFO's powered assistance within a training session by employing altered muscle commands while wearing the robot on the paretic leg, and whether such alterations can be accounted for by changes in the underlying muscle synergies. From a rehabilitation point of view, we ideally expect such AFO-induced alterations of muscle synergies to be towards the direction of restoring the normal synergies used by unimpaired individuals for walking.

## MATERIALS AND METHODS

### Study Participants

Chronic stroke survivors (8 males, 2 females;  $60.20 \pm 5.65$  [mean  $\pm$  SD] years old;  $6.91 \pm 4.94$  years post-stroke; **Table 1**) were recruited from the community on a voluntary basis. Subjects were eligible for inclusion if they had (1) unilateral stroke  $\geq 12$  months prior to enrolment; and (2) mild to moderate motor impairment that allowed them to walk without manual assistance, with or without the support of a cane. All subjects gave written informed consent before experimentation. All procedures of this study were reviewed and approved by the Joint Chinese University of Hong Kong – New Territories East Cluster Clinical Research Ethics Committee and were conducted in accordance with the Declaration of Helsinki.

Patient ID	Gender (F/M)	Age (years)	Time since stroke (years)	Affected Side	BBS	FMA-LE*
CS01	M	62	9.08	Left	18	48
CS02	M	67	1.92	Right	20	46
CS03	M	52	16.00	Right	21	50
CS04	M	67	5.58	Left	16	41
CS05	M	52	2.42	Right	16	41
CS06	F	59	2.17	Right	16	41
CS07	M	60	3.00	Right	24	38
CS08	M	64	9.50	Right	24	53
CS09	F	55	14.42	Left	19	50
CS10	M	64	4.00	Right	16	50
<b>Mean</b>	<b>F (2/10)</b>	<b>60.20 <math>\pm</math> 5.65</b>	<b>6.91 <math>\pm</math> 4.94</b>	<b>R (7/10)</b>	<b>19 <math>\pm</math> 3.20</b>	<b>45.8 <math>\pm</math> 5.16</b>

**Table 1.** Demographics and clinical characteristics of the chronic stroke survivors recruited in this study.

### The Experimental Protocol

**The Ankle Robot Exoskeleton.** Gait training was conducted with an ankle robotic exoskeleton that provided assistive torque on the stroke-affected lower limb. Our device consisted of a light-weight, unilateral powered ankle foot orthosis previously developed by a team from The Chinese University of Hong Kong and The Hong Kong Polytechnic University (Yeung et al. 2017). The ankle robot was composed of an assistive motorized brace (weight of  $\sim 0.5$  kg) that was fixed at the user's shank, and a control box with a LiPo battery system ( $\sim 0.5$  kg) secured at the user's waist. The device's control algorithm predicted the next motion of the wearer, and subsequently generated a modulated assistive torque based on this prediction to support ankle joint movements during over-ground gait. Details of the wearable's control algorithm can be found in Yeung et al. (2017).

**Exoskeleton-Based Gait Training.** Within one single training session, subjects walked over-ground along a 4.50-m walkway in 3 consecutive epochs, in the following order: a) unperturbed-unassisted walking, executed without wearing the exoskeleton ('**exo-FREE**', or **FREE**); b) perturbed-unassisted walking, performed wearing the exoskeleton with its power-assistive function turned off ('**exo-OFF**', or **OFF**); c) perturbed-assisted walking, performed wearing the exoskeleton with its power-assistive function turned on ('**exo-ON**', or **ON**). These 3 conditions were designed to separately reveal the effects exerted on the muscle synergies by two distinct kinds of limb perturbations introduced by the ankle robot: *perturbation 1*, exerted by the weight and the wearing

of the robot itself without the assistive torque, assessed by comparing *exo-OFF* vs. *exo-FREE*; *perturbation 2*, exerted by the assistive torque of the robot, and assessed by comparing *exo-ON* vs. *exo-OFF*.

For each of the 3 epochs, subjects were asked to walk along the entire length of the walkway for 10 times. For safety reasons, they were free to walk at their self-selected, comfortable speeds, and to ask for breaks or stop the trial whenever they deemed necessary.

**Data Collection.** During training, electromyographic signals (EMGs) were simultaneously recorded from 28 lower-limb and trunk muscles on both the paretic and non-paretic sides, with 14 muscles per side. Wireless EMG sensors (Trigno System, Delsys, Boston, MA, USA; and Noraxon wireless system, Noraxon, Scottsdale, AZ; sampling frequency of 1000 Hz) were placed according to SENIAM recommendations (Hermens et al. 2000), to the extent possible, to record the activities of the following muscles on each side: latissimus dorsi (LD), erector spinae (ES), external oblique (EO), gluteus maximus (GM), tensor fascia latae (TFL), adductor longus (AL), hamstrings (Hams), vastus medialis (VM), vastus lateralis (VL), rectus femoris (RF), medial gastrocnemius (MGA), lateral gastrocnemius (LGA), soleus (Sol), and tibialis anterior (TA). Gait-cycle events and gait speed were detected by a motion capture system consisting of 10 infrared cameras (VICON Vantage V5, Oxford Metrics Group Ltd., Oxford, UK; sampling rate of 100 Hz), which tracked the 3D motion of reflective markers (diameter of 14 mm) placed on the heel surface. The EMG and motion capture systems were time synchronized.

**Clinical Assessments.** Balance and motor abilities of all stroke survivors were assessed by clinical scores including the Berg Balance Scale (BBS) (Berg et al. 1992) and Fugl-Meyer Assessment (Fugl-Meyer et al. 1975) for Lower-Extremities (FMA-LE). In order to reduce the assessment time and prevent subsequent fatigue of the patients, when measuring FMA-LE we decided to focus on impairment features related to lower-limb joint motions, and thus measured only the assessment's sub-scores related to flexion and extension abilities of the hip, knee, and ankle joints (FMA-LE\*, maximum score = 30; see Supplementary Materials, Table S1).

## **Analysis Workflow**

**Segmentation and Selection of the Recorded Data.** The raw EMGs were first visually inspected, and the trials or channels showing poor signal quality were discarded. The remaining data were then segmented into gait cycles. A step cycle is defined here as the time interval between two consecutive heel strikes of the same limb. Trajectories of the heel markers were reconstructed in the Vicon Nexus environment for the identification of all heel strike moments.

In our analysis, we aimed to characterize how stroke survivors adjusted their gait to adapt to the *exo-OFF* and *exo-ON* perturbations. In order to exclusively analyse the steps with presumably the highest level of adaptation to the exoskeleton attained within the epochs with perturbations, for the *exo-OFF* and *exo-ON* epochs we only analysed, for the paretic side, the gait cycles belonging to the last ~30% of the epoch (Houldin et al 2011, Steele et al. 2017). In addition, among these selected cycles, we only considered the steps performed over the middle part of the walkway by dropping the first and last cycles of each walkway trial, since the steps associated with starting or stopping a multi-step episode could be characterized by very different kinematics (Kibushi et al. 2018, Mbourou et al. 2003). With these rather stringent selection criteria, we obtained an average of ~10

step cycles for each perturbation epoch of each subject. This sample size of step cycles was deemed sufficient for downstream analysis, because per previous studies (Schiavi et al. 1998), a minimum of 6 to 10 strides are usually needed to reconstruct a representative EMG profile.

***EMG Pre-processing and Muscle Synergy Extraction.*** The selected raw EMGs of each muscle were high-pass filtered (4th order Butterworth filter, cut-off frequency of 40 Hz), rectified, low-pass filtered (4th order Butterworth filter, cut-off frequency of 10 Hz), integrated over 20-ms intervals, and variance-normalized (Cheung et al. 2009). Then, to facilitate subsequent comparisons between the paretic and non-paretic sides and across epochs, we organized the pre-processed EMGs of each subject into 7 data matrices – denoted by  $\mathbf{M}_i$ ,  $i \in \{0,1,\dots,4,123,1234\}$  (Table 2) – by selecting and recombining portions of the EMGs in different ways. The logic and purpose of such groupings will become apparent as the analytic procedures are explained in the next paragraphs.

Time-invariant muscle synergies were extracted from *each* of the resulting EMG matrices,  $\mathbf{M}_i$  (Table 2), using the standard Non-Negative Matrix Factorization (NNMF) algorithm (Lee and Seung 1999). As is well known, in the NNMF model, EMGs are generated according to the following model,

$$\mathbf{D} = \mathbf{W}\mathbf{C} + \boldsymbol{\varepsilon}; \mathbf{D}, \mathbf{W}, \mathbf{C} \geq 0;$$

where  $\mathbf{D}$  is the matrix containing time-series activities of multiple muscles (as row vectors),  $\mathbf{W}$  is a matrix of muscle synergies (as column vectors),  $\mathbf{C}$  is the time-dependent coefficients for the synergies (as row vectors), and  $\boldsymbol{\varepsilon}$  is any residual activities unexplained by the model. In other words, the time-invariant muscle synergies are “activated” by time-varying coefficients, and then linearly combined to generate multi-muscle EMG activities.

For every data matrix, the NNMF algorithm was applied 14 times with the number of synergies extracted set to 1 to 14 (the number of recorded muscles on each side), respectively. For each of the 14 extractions, the NNMF was run 20 times, and the solution associated with the highest EMG-reconstruction  $R^2$  analysis was selected for further examinations.

To determine the “correct” number of muscle synergies – or dimensionality – of each of the  $\mathbf{M}_i$  matrices, we first focused on the matrix with EMGs from the non-paretic side ( $\mathbf{M}_0$ ), and identified, among the 14 synergy sets, the minimum dimensionality that yielded an  $R^2 \geq 0.75$  (Coscia et al. 2014). This minimum was then set as the correct dimensionality for  $\mathbf{M}_0$ , and the precise EMG-reconstruction  $R^2$  attained for  $\mathbf{M}_0$  at this dimensionality was then used as a reference for determining the dimensionality of the other  $\mathbf{M}_i$  matrices, as follows. For each  $\mathbf{M}_i$ , the number of synergies that yielded a minimum of  $|\mathbf{R}_{\text{non-paretic (selected set)}}^2 - \mathbf{R}_{\text{paretic}}^2|$  was selected as the matrix’s dimensionality. This way, we could ensure that the selected dimensionalities would not be biased into describing some matrices better than the others because the  $R^2$  of the same  $\mathbf{M}_0$  reference was used for all matrices related to the paretic side.

***Across-epoch Comparison of Muscle Synergies from the Same Limb.*** Whether the muscle synergies  $\mathbf{W}$  of the paretic side were altered across the 3 walking epochs was explored by two complementary approaches, named here ‘*constant W*’ and ‘*variable W*’. The *constant-W* approach evaluated the hypothesis that, the number and muscular compositions of all muscle synergies are preserved across epochs; thus, any changes in EMGs in exo-OFF and exo-ON are attributable to

changes in the synergies' activation coefficients,  $\mathbf{C}$ . For this analysis, the  $\mathbf{W}$  matrix was first set as constant across the entire data set recorded from the last 30% of exo-FREE, exo-OFF, and exo-ON as  $\mathbf{W}$  was extracted from matrix  $\mathbf{M}_{123}$  (Table 2). Then, the validity of the obtained  $\mathbf{W}$  was investigated by examining the EMG-reconstruction  $R^2$  of every individual step cycle. If the constant- $\mathbf{W}$  model is valid, the cycle- $R^2$  values from this extraction should be similar across epochs; otherwise, one or two of the epochs would show higher or lower cycle- $R^2$  values.

The potential presence, across epochs, of significant alterations in the number and/or structures of  $\mathbf{W}$  was further investigated by the *variable-W* approach – i.e., by comparing synergy sets extracted independently from exo-FREE ( $\mathbf{M}_1$ ), exo-OFF ( $\mathbf{M}_2$ ) and exo-ON ( $\mathbf{M}_3$ ) matrices. Similarity of  $\mathbf{W}$  between any two epochs was assessed by the best-matching scalar product (SP) after the magnitude of every muscle-synergy vector was normalized, as described in earlier works (Cheung et al. 2012). The higher the SP between any two muscle synergies, the more similar they are in muscular composition.

***Defining Reference Scalar Product Values for Assessing Synergy Similarity.*** As outlined above, in our variable- $\mathbf{W}$  approach the across-epoch similarity of  $\mathbf{W}$  was quantified by SP values. To ascertain whether an SP value indicates a significant change in  $\mathbf{W}$  beyond what is expected from its expected variability, reference SP values were obtained by comparing synergy sets extracted independently from 2 non-overlapping portions of exo-FREE. These control reference values allowed us to quantify the expected variability of  $\mathbf{W}$  across different unperturbed steps in the absence of exoskeleton, which may be caused by noise, the inability of the NNMF in discovering the solution for  $\mathbf{W}$  at the global extremum, or the natural physiological inter-step variability of muscle activations. To maximize  $\mathbf{W}$  variations in our SP references, we specifically compared the synergies extracted from the last ~30% of exo-FREE ( $\mathbf{M}_1$ ) with the ones extracted from the most temporally distant set of steps performed within the same walking epoch – i.e., the initial 10 steps ( $\mathbf{M}_4$ ). Only SP changes that were higher than our reference SP as defined above were considered as values that reflect significant  $\mathbf{W}$  changes attributable to the exoskeleton.

***Across-epoch Comparison of the Time-Varying Activation Coefficients of the Paretic-side Synergies.*** For the paretic-side muscle synergies that remained invariant across the unperturbed and perturbed epochs, their time-varying activation coefficients ( $\mathbf{C}$ ) were compared across epochs. For any synergies whose  $\mathbf{C}$ 's are being compared, their associated  $\mathbf{W}$ 's must ideally remain fixed across epochs so that the  $\mathbf{C}$ 's being compared would represent activation trajectories in a subspace spanned by an identical set of basis vectors (i.e., the muscle synergies). In order to achieve this, the conserved- $\mathbf{W}$  approach was first applied to matrix  $\mathbf{M}_{1234}$  in order to extract a fixed  $\mathbf{W}$  across all epochs. To identify the subset of  $\mathbf{W}$  that was preserved, each synergy from  $\mathbf{M}_{1234}$  was then compared with the synergy set obtained for each individual epoch from the variable- $\mathbf{W}$  approach. A constant- $\mathbf{W}$  synergy was considered invariant if, for *all* epochs, its best-matching SP to the epoch-specific variable- $\mathbf{W}$  synergy was higher than a similarity threshold. This threshold was calculated according to a previously described method (Cheung et al. 2009, García-Cossio et al. 2014) – i.e., by corrupting each synergy from constant- $\mathbf{W}$  with a random Gaussian noise ( $\mu = 0$ ,  $\sigma = 0.1$ ; 1000 repetitions), and finding the average SP between all pairs of noise-corrupted synergies. This average

SP was then used as the synergy’s similarity threshold. The **C**’s corresponding to the invariant **W**’s obtained from the constant-**W** extraction were then compared across epochs.

For each conserved synergy, its **C**’s for every step cycle was interpolated into 200 time points and averaged across cycles. Similarity between the averaged **C**’s of any two epochs was quantified by the Pearson’s correlation coefficient ( $r$ ). Similar to the **W** analysis, when assessing the across-epoch similarity of the activation coefficients, reference values of  $r$  were obtained by comparing the **C**’s from two non-overlapping portions of exo-FREE. Following Mukaka (2012), the  $r$  threshold above which the  $r$  was considered to indicate a strong correlation was set to 0.70.

**Inter-Side Comparison of Muscle Synergies.** The potential changes in similarity between the muscle synergies of the paretic and non-paretic legs across the 3 walking epochs was assessed by comparing the number and structures of synergies from the paretic data matrices (**M**<sub>1</sub>, **M**<sub>2</sub> and **M**<sub>3</sub>) with those from the non-paretic matrix (**M**<sub>0</sub>). Importantly, here the non-paretic synergies that served as a “baseline reference” were exclusively obtained from the EMGs of the exo-FREE condition (**M**<sub>0</sub>), considering that wearing of the exoskeleton may potentially alter the muscle activation patterns even of the non-paretic side. Since the assistive torque of the exoskeleton represents the actual intervention provided for improving gait kinematics, we are particularly interested in comparing exo-OFF vs. exo-ON so as to understand the effect of the assistive torque *per se* (i.e., *perturbation 2*) on the inter-side muscle-synergy similarity.

<b>Data matrix</b>	<b>Description</b>
<b>M</b> <sub>1</sub>	Processed paretic EMGs from exo-FREE
<b>M</b> <sub>2</sub>	Processed paretic EMGs from exo-OFF
<b>M</b> <sub>3</sub>	Processed paretic EMGs from exo-ON
<b>M</b> <sub>123</sub>	Processed paretic EMGs recorded from exo-FREE + exo-OFF + exo-ON
<b>M</b> <sub>4</sub>	Processed paretic EMGs recorded from the first 10 step-window of exo-FREE
<b>M</b> <sub>1234</sub>	Processed paretic EMGs recorded from exo-FREE (first and last step-window) + exo-OFF + exo-ON
<b>M</b> <sub>0</sub>	Processed non-paretic EMGs from exo-FREE

**Table 2.** Description of the 7 data-matrices obtained from the processing of the experimental raw-EMGs. From these matrices, synergy sets have been iteratively extracted for the inter- and intra-side analysis.

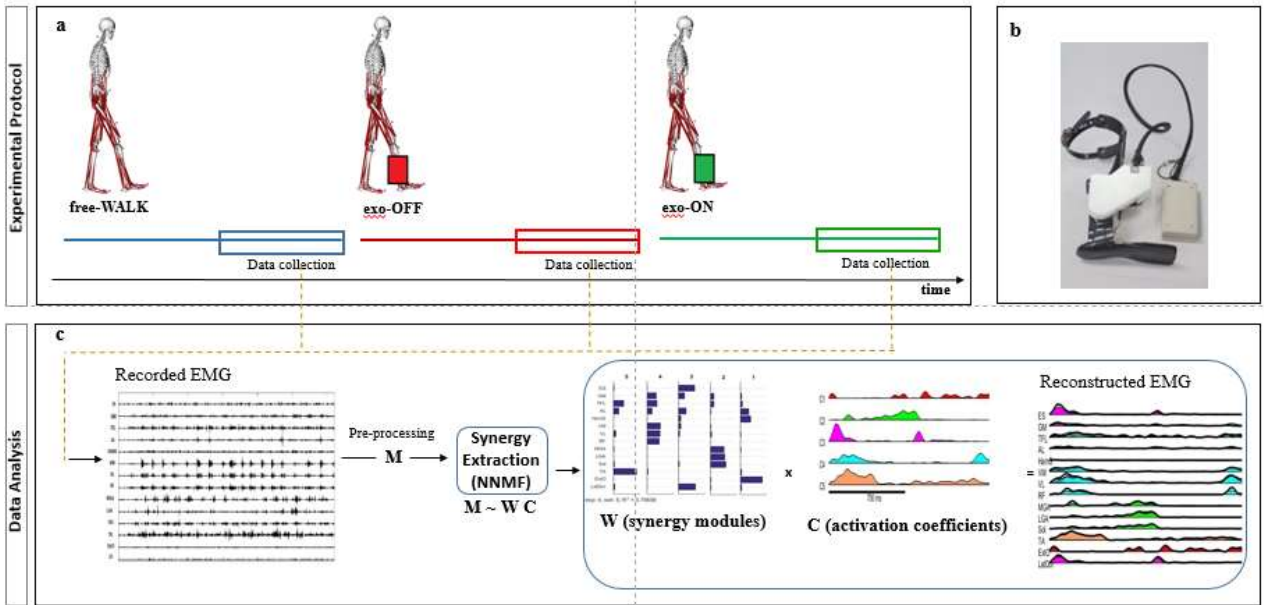


**Fig. 1. Schematic Representation of the Experimental and Synergy Analysis Procedure Adopted in this Study.** Panel a. Representation of the gait training protocol adopted, consisting in the 3 consequent walking sessions exo-FREE, exo-OFF and exo-ON, with the 3 related data-collection windows for synergy extraction (last third portion of each session). Panel b. The Ankle Robot under investigation. Panel c. The main analysis workflow adopted for the synergy extraction procedure, starting from the input (experimental raw-EMGs) to the final output (synergy factors  $W$  and  $C$ ). From the output, the reconstructed-EMG =  $W \cdot C$  can be obtained. Skeletal figures in panel a were created in OpenSim environment (Delp et al., 2007).

**Correlation between Synergy Alterations and Clinical Scores.** The across-epoch changes in inter-side synergy similarity, quantified by differences in SP values, were correlated to the subjects' clinical scores including BBS, FMA-LE\*, and their linear summation. This linear summation was formulated as a customized clinical index (named here 'Global Clinical Index', or GCI) that summarizes the balance and motor abilities of stroke survivors:

$$GCI = (FMA-LE^*/Max FMA-LE^* + BBS/Max BBS)/2,$$

where Max FMA-LE\* is equal to 30, and Max BBS, to 56.

The degree of correlation between the synergy- and clinical-related variables was assessed by the Pearson's correlation coefficient  $r$ .

## Statistics

Descriptive statistics were performed for evaluation of the mean and standard deviation (SD) of the variables obtained from the analysis. Paired student's t-tests and Repeated measures ANalysis Of Variance (RANOVA) were implemented to statistically evaluate hypotheses concerning the changes in the number, structures, and temporal activations of the muscle synergies across epochs. In cases when the tests' normality assumption was not met, their corresponding non-parametric tests were used. Significance level ( $\alpha$ ) was set to 0.05.

## RESULTS

### The constant-W muscle synergy model

#### *The constant-W model failed to describe the EMGs of the 3 walking epochs equally well.*

We first assessed to what extent the muscle synergies,  $\mathbf{W}$ , of the paretic leg were preserved across the 3 walking epochs (exo-FREE, exo-OFF, and exo-ON) by examining whether the constant-W model (see Methods) could explain the step cycles of all epochs equally well. The constant-W model, in which  $\mathbf{W}$  was locked across the 3 epochs, allowed us to identify an EMG dimensionality (i.e., number of muscle synergies) of  $6 \pm 0.471$  (mean  $\pm$  SD) across subjects. A statistically significant difference between the mean EMG-reconstruction  $R^2$  values for the steps of exo-FREE, exo-OFF and exo-ON was detected ( $P=0.013$ , Repeated measures-ANOVA, Fig. 2).

From this result, we could not assume that the EMG variability of the 3 walking epochs could be equally well captured by a single set of invariant muscle synergies,  $\mathbf{W}$ . In other words, any EMG changes elicited by either the wearing of the exoskeleton *per se* and/or the robot's assistive torque could *not* just be attributed to changes in the synergies' temporal activation coefficients ( $\mathbf{C}$ ).

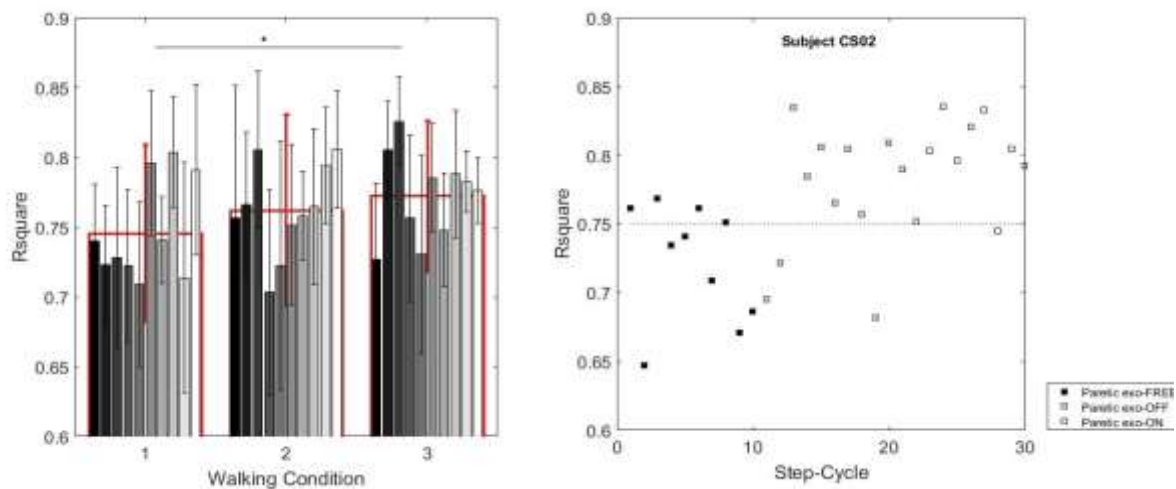


**Fig. 2.  $R^2$  reconstruction analysis associated with the conservative  $\mathbf{W}$  model. Panel a.** Bars represent the  $R^2$  values (mean  $\pm$  SD) associated with each single step of the  $\mathbf{M}_{123}$  matrix, grouped according to each of the 3 walking conditions exo-FREE, exo-OFF and exo-ON. Red-coloured bars represent the mean values ( $\pm$  SD)/walking condition. Statistically significant difference was detected between the 3 conditions ( $P=0.013$ , Repeated-Measures ANOVA). **Panel b.**  $R^2$  values associated with each of the selected steps performed by one specific patient. We observed a significant increase in the quality of the EMG reconstruction between exo-FREE and exo-ON ( $P=0.0009$ , Repeated-Measures ANOVA). (\* symbol indicates  $P<0.05$ ).

### The variable-W muscle synergy model

#### *Robotic assistive torque elicited additional muscle synergies on the paretic leg in some subjects.*

In exo-FREE, in the absence of any exoskeletal perturbation, the number of muscle synergies on the paretic side differed from that for the non-paretic baseline by at most 1 ( $\Delta n = \pm 1$ ) across stroke survivors (Fig. 3C). In fact, for exo-FREE no statistically significant difference between the mean

numbers of muscle synergies for the non-paretic and paretic sides was found ( $P=0.072$ , paired t-test), and the numbers of synergies for both sides was always within the range of 5 to 6.

However, across the 3 epochs, as exoskeletal perturbations were introduced, there was a progressive increase in the number of subjects reporting a dimensionality of 6 synergies on the paretic side: from 40% in exo-FREE, to 50% in exo-OFF, and then 60% in exo-ON. The higher percentage of subjects with 6 synergies when assistive torque was present led to a significant difference, in exo-ON, between the mean number of synergies on the paretic side and that for the non-paretic reference, with the paretic side possessing more synergies (mean  $n_{\text{non-paretic}} = 5.1$  vs. mean  $n_{\text{exo-ON}} = 5.6$ ,  $P=0.015$ , paired t-test, Fig. 3B). Per previous studies (Nishida et al. 2017, Yokoyama et al. 2016), an increase in the number of lower-limb synergies correlated well with higher gait speeds; thus, we also performed a kinematic analysis to evaluate the differences in gait speed between the 3 epochs. Since no significant difference was found across the mean speeds of the epochs (Fig. 4,  $P=0.462$  Repeated-Measure ANOVA), we ruled out the possibility that the additional synergies in exo-OFF and exo-ON were induced by the adoption of faster walking speeds.

We note here that the additional muscle synergies observed in exo-ON included significant activation components in muscles tibialis anterior (TA) and external oblique (EO) (Fig. 6D, Fig. 7B, Fig. 7C). Importantly, the increase in the number of muscle synergies in exo-ON appeared to be the result of uncoupling abnormally merged muscle synergies that is associated with post-stroke motor impairment (Clark et al. 2010, Cheung et al. 2012), and was observed in those subjects during unperturbed walking (Fig. 7). Indeed, the additional exo-ON synergies involved individuated activations of TA and EO. Muscle TA was abnormally coupled with tensor fasciae latae (TFL) in exo-FREE, but regained its independence in exo-ON. Similarly, EO was coupled with latissimus dorsi (LD) in exo-FREE, and became independent in exo-ON.

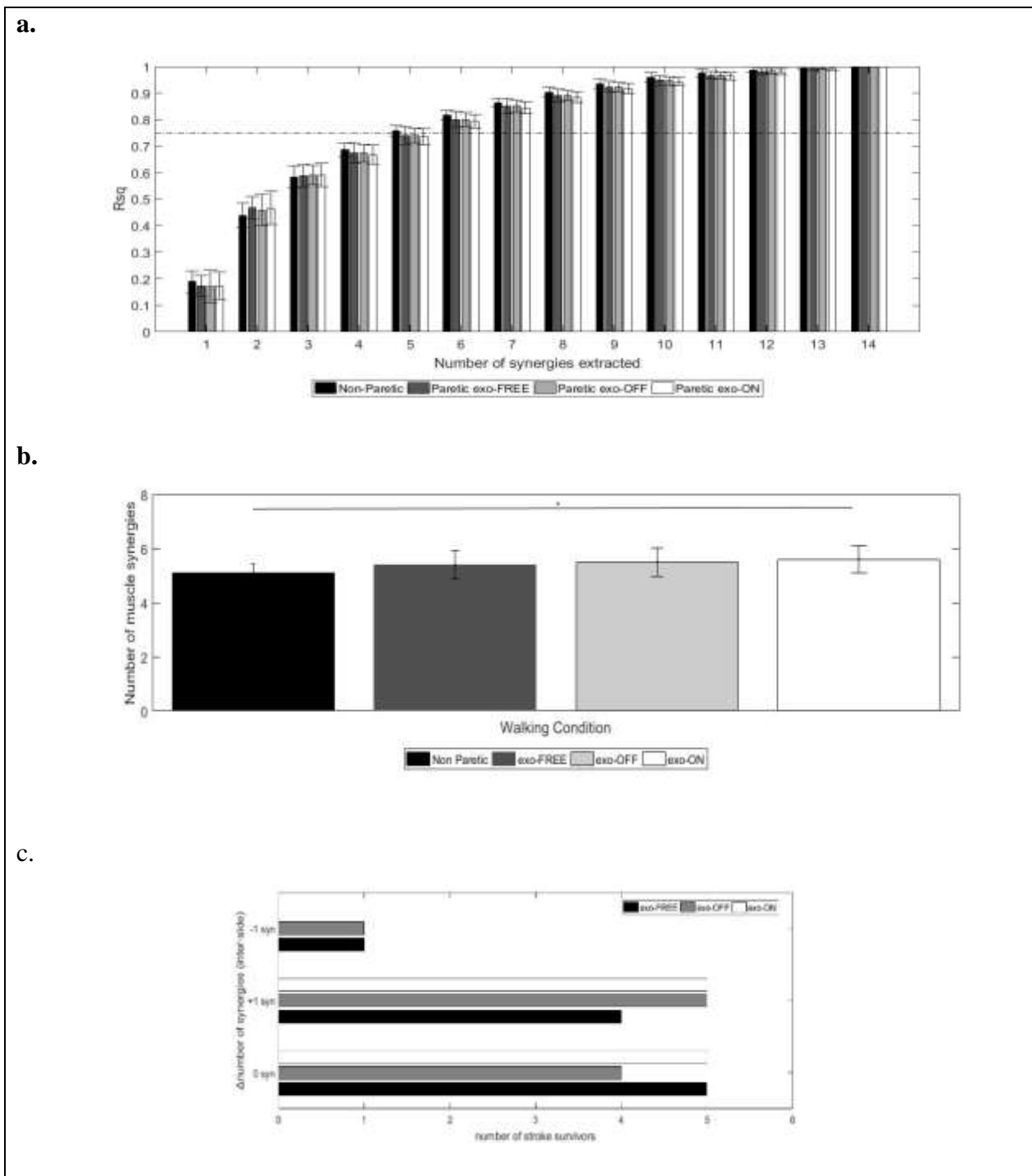


**Fig. 3. Dimensionality of the Synergy Space across Walking Conditions.** Panel a.  $R^2$  reconstruction analysis associated with the Variable W model. Bars represent the  $R^2$  values (mean  $\pm$  SD) associated with each of the 14 best synergy set obtained from the NMF run (n. synergies set to 1:14) for the non-paretic side reference (from matrix  $M_0$ ), the paretic exo-FREE (matrix  $M_1$ ), paretic exo-OFF (matrix  $M_2$ ) and paretic exo-ON (matrix  $M_3$ ) analysis. The dotted horizontal line represents the  $R^2$  threshold = 0.75 adopted for the synergy set's selection. Panel b. Number of synergies (average  $\pm$  SD) extracted from the non-paretic (exo-FREE) and paretic side (exo-FREE, exo-OFF and exo-ON) ( $P=0.015$  between paretic exo-ON and non-paretic ref. pairs, paired t-test). Panel c. Inter-side changes in the number of synergies across exo-FREE (black colour), exo-OFF (grey colour) and exo-ON (white colour).

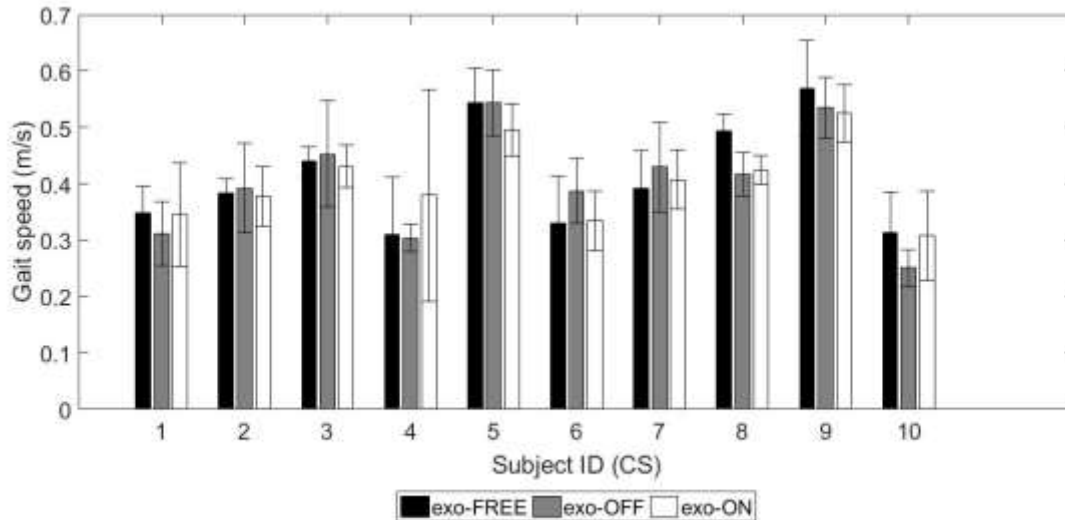


**Fig. 4. Gait speed across the three walking conditions.** Gait speed ([m/s], average  $\pm$  SD) adopted by each of the 10 study participants during the 3 walking sessions exo-FREE, exo-OFF and exo-ON. No statistical significance ( $\alpha$ -level = 0.05) was found inter-condition between the 3 mean speeds ( $P=0.463$ , Repeated-Measure ANOVA).

***Robotic exoskeleton altered the muscle synergies of the paretic leg.***

We next sought to reveal how the perturbing forces from the exoskeleton altered the muscle synergies on the paretic side by comparing the paretic-side synergies between the different epochs. Similarity between any two sets of synergies was quantified first by finding the best-matching scalar product (SP) values between the matched synergy pairs, and then calculating the mean and minimum SPs across the pairs. The minimum SP indicates the similarity of the least similar synergy pair after matching.

To assess the overall effect of the active exoskeleton, we first compared the synergies of exo-FREE vs. those of exo-ON. Across subjects, the mean SP in this comparison ( $0.890 \pm 0.055$ ) was significantly lower than the baseline reference mean ( $0.950 \pm 0.037$ ) obtained from non-overlapping portions of the exo-FREE steps ( $P = 0.014$ , Wilcoxon signed rank test; Fig. 5). The same relationship is also to be said for the minimum SP (exo-ON vs. exo-FREE,  $0.621 \pm 0.281$ ; baseline within exo-FREE,  $0.871 \pm 0.113$ ;  $P = 0.020$ ; Fig. 5).

Then, to assess whether the wearing of the exoskeleton itself, *without* any assistive force, was sufficient to induce changes in **W**, we compared the synergies of exo-FREE vs. those of exo-OFF. This comparison in fact yielded the lowest mean SP ( $0.871 \pm 0.072$ ; comparison with exo-FREE baseline,  $P = 0.037$ ) and minimum SP ( $0.596 \pm 0.274$ ;  $P = 0.027$ ) obtained among all of our comparisons. Thus, even the inactive exoskeleton contributes considerably to changes in **W** induced during our intervention.

Finally, to assess changes induced just by the assistive torque, we compared the synergies of exo-OFF vs. those of exo-ON. When compared with the degree of change from exo-FREE to exo-OFF, the extent of **W** change on the paretic side from exo-OFF to exo-ON was relatively modest. The minimum SP associated with this change appeared to be low in magnitude ( $0.651 \pm 0.322$ ) but was

found to be not significantly different from the degree of change expected during the exo-FREE baseline ( $P = 0.193$ , Wilcoxon signed rank test). The same is to be said for the mean SP value ( $P = 0.160$ ).

Taken together, our comparisons presented above suggest that the perturbative forces introduced by the active exoskeleton led to significant alterations of the muscular compositions of the muscle synergies ( $\mathbf{W}$ ) on the paretic side (Fig. 5). However, the largest degree of  $\mathbf{W}$  changes may be due to the wearing of the exoskeleton *per se* – either from its weight as an inertial load, or from the reactions driven by the cutaneous activations resulting from the wearing – rather than from the assistive torque generated by the ankle robot, both because the FREE-vs-OFF SP was lower than the OFF-vs-ON SP, and because the FREE-vs-ON SP was not significantly different from the FREE-vs-OFF SP. At this point, it should be noted that the relatively modest OFF-to-ON changes in  $\mathbf{W}$  does not necessarily imply that such changes are not functionally significant, as will be apparent in the next sections.

We note that overall, TA was the paretic-leg muscle most involved in the changes of synergies across the three walking epochs. It was an active muscle (component weight of 0.3 to 1 after normalization of synergy-vector magnitude) in 46% of the altered muscle synergies (latter epoch) having low inter-epoch SP values ( $SP < 0.70$ ). In some altered synergies its component weight peaked at  $\sim 0.96$  to  $0.98$  (Fig. 6A-C). Other muscles involved in synergy changes included the hamstrings (Ham) and gluteus maximus (GM) muscles, active (component weights  $>0.3$ ) in 30% of the altered synergies in the latter epoch. The involvement of TA and Ham was particularly evident over the OFF-to-ON transition; they showed significant weights ( $>0.95$ ) after the assistive power was turned on in 3 of the 4 instances (Fig. 6C). In addition, muscle EO was a trunk muscle that was noted in some instances. Other muscles, such as gastrocnemius and the vastus muscles, were active in the altered synergies in  $\leq 15\%$  of the instances of alteration.

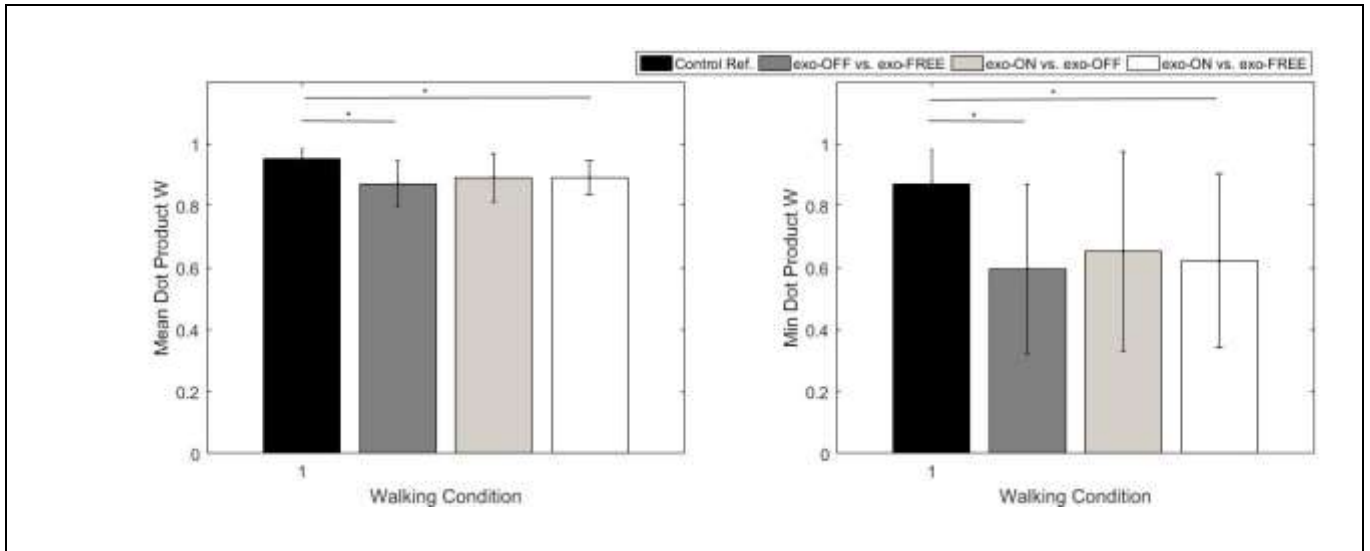


**Fig. 5. Similarity of synergies W across walking conditions.** Panel a. Mean SP and min SP/subject (average  $\pm$  SD) of the 10 stroke survivors. The symbol \* indicates  $P < 0.05$ .

Subject ID	Min SP / subject set Control References	Min SP / subject set 'exo-OFF' vs 'exo-FREE'	Min SP / subject set 'exo-ON' vs 'exo-OFF'	Min SP / subject set 'exo-ON' vs 'exo-FREE'
subj CS01	0.980	0.558	0.441	0.946
subj CS02	0.967	0.540	0.603	0.072
subj CS03	0.914	0.979	0.731	0.713
subj CS04	0.724	0.081	0.948	0.202
subj CS05	0.815	0.850	0.914	0.830
subj CS06	0.647	0.734	0.897	0.761
subj CS07	0.897	0.716	0.796	0.523
subj CS08	0.952	0.578	0.222	0.789
subj CS09	0.967	0.210	0.033	0.614
subj CS10	0.842	0.715	0.926	0.759

**Table 3.** Single values of inter-condition min SP (per subject-set) associated to each of the 10 stroke survivors.

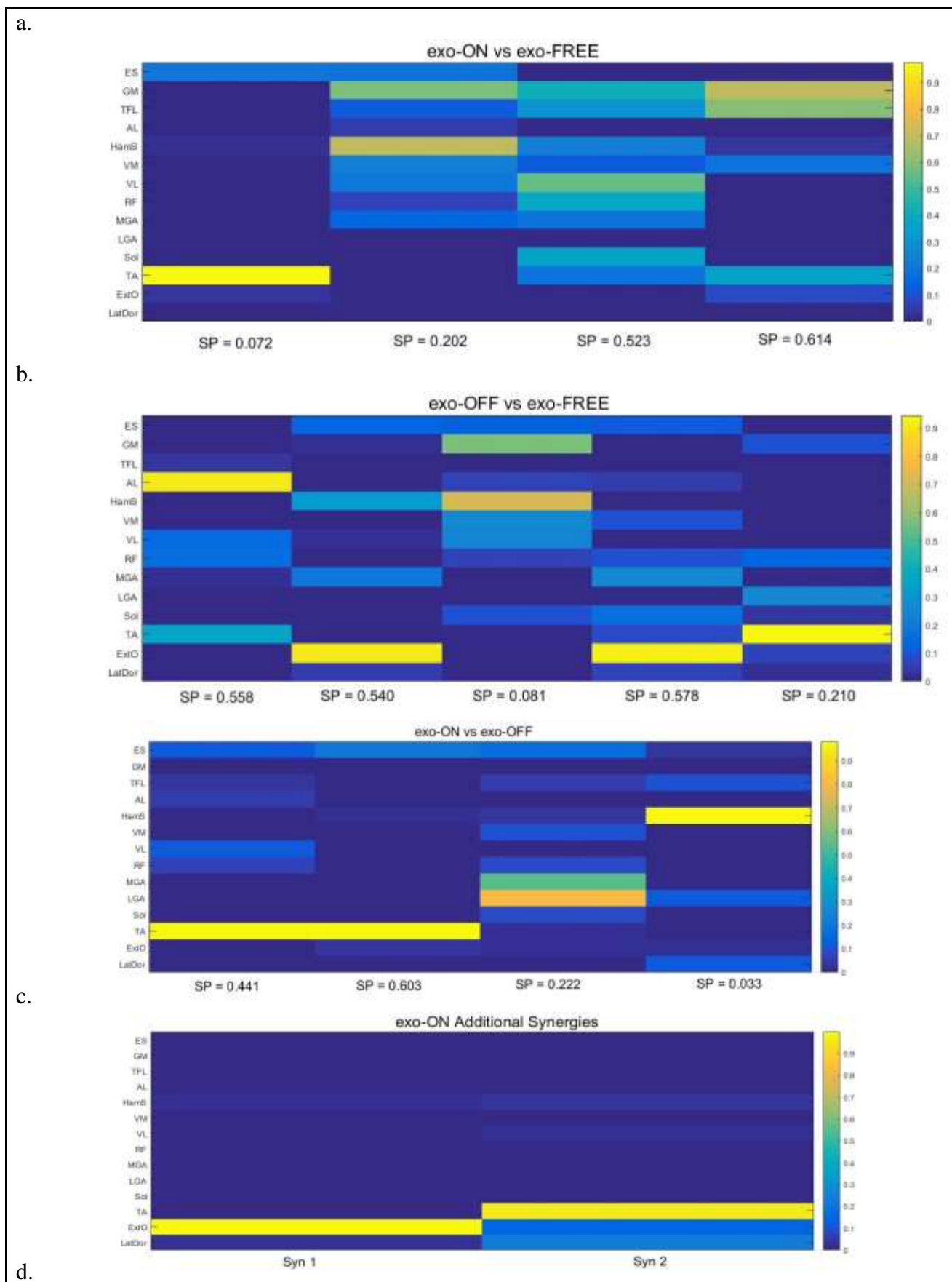


**Fig. 6.** Panel a-c. Synergies showing low SP values in the inter-epoch comparisons (exo-ON synergies vs exo-FREE in panel a, exo-OFF synergies vs exo-FREE in panel b, exo-ON synergies vs exo-OFF in panel c). Panel d. Additional synergies associated with exo-ON epoch.

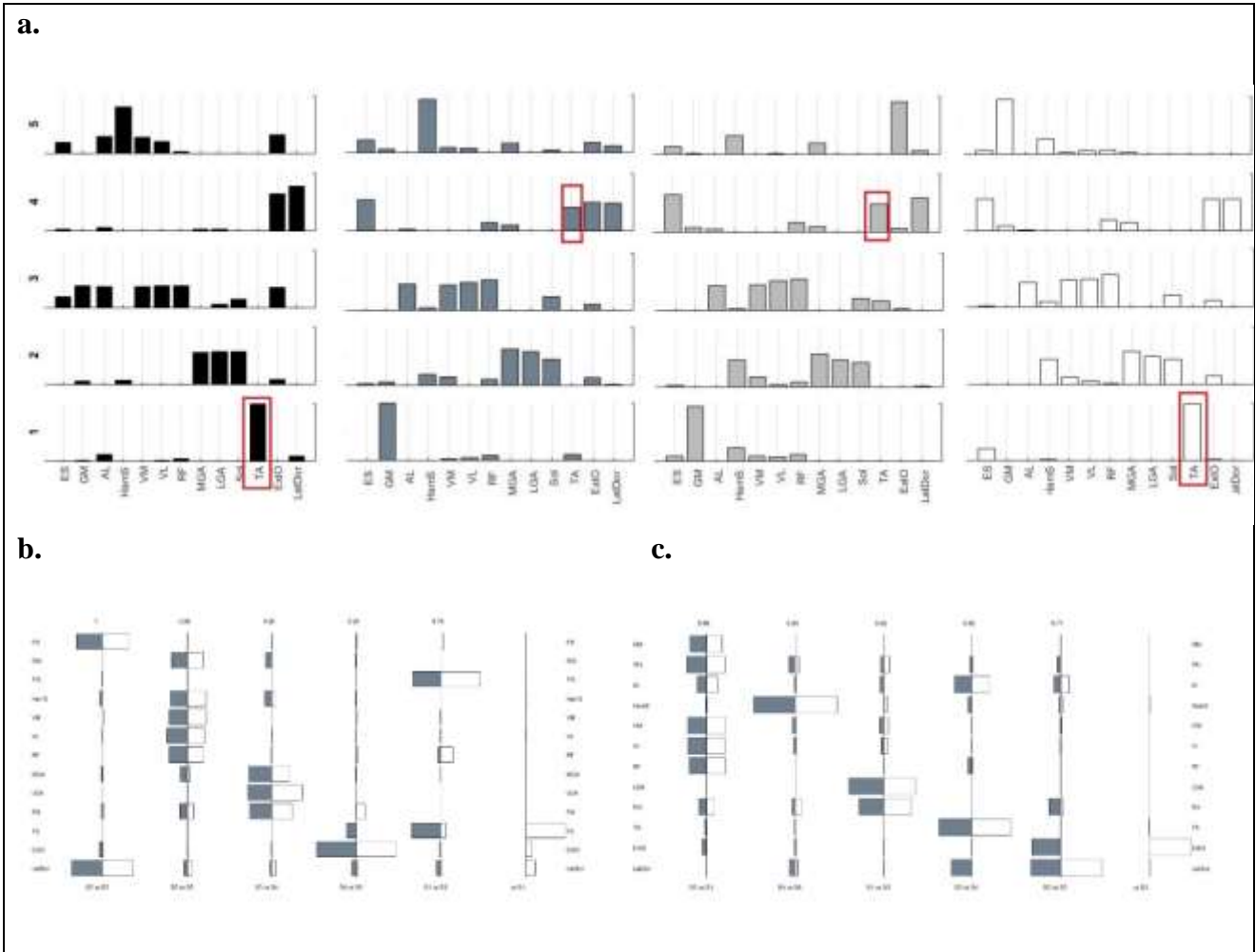


**Fig. 7.** Panel a. Example of changes in synergy sets across walking conditions in one specific patient. Reference synergies from non-paretic side are in black colour, paretic-free-WALK-synergies in dark-grey, paretic-exo-OFF in light-grey, paretic-exo-ON in white colour.. Panel b and c. Pairs of synergy sets showing the additional synergy introduced with exo-ON.

***Concomitant changes in the synergies' temporal activations were observed across walking epochs.***

After examining across-epoch changes in  $\mathbf{W}$ , we proceeded to analyse across-epoch changes in the synergies' temporal activation coefficients, the  $\mathbf{C}$ , through a similar strategy of comparison. Cycle averages of the  $\mathbf{C}$  of each synergy were computed after re-sampling each step cycle into 200 time points. Similarity of the  $\mathbf{C}$  between any two epochs was quantified by the Pearson's correlation coefficient ( $r$ ).

In our exo-FREE vs. exo-ON comparison, the exoskeleton had a significant effect on the  $\mathbf{C}$ 's of the paretic-side synergies. Both the mean  $r$  ( $0.685 \pm 0.087$ ) and minimum  $r$  ( $0.401 \pm 0.20$ ) were, in fact, smaller than our predefined threshold of  $\mathbf{C}$  similarity (0.70). Statistical analysis showed that they were also significantly smaller than the  $r$  expected from the variability of the baseline exo-FREE steps on the non-paretic side ( $P = 0.002$  for mean  $r$ ,  $P = 0.049$  for minimum  $r$ , Wilcoxon signed rank test; Fig. 8A).

Similar to the **W** analysis, the FREE-vs-OFF comparison showed lower **C** correlation levels than the OFF-vs-ON comparison. For OFF-vs-ON, both the mean  $r$  ( $0.793 \pm 0.067$ ) and minimum  $r$  ( $0.569 \pm 0.168$ ) were not significantly different from the expected  $r$  in the non-paretic-side baseline control ( $P = 0.695$  for mean  $r$ ,  $P = 0.431$  for minimum  $r$ , Wilcoxon signed rank test). Despite this lack of statistical significance from OFF to ON, heterogeneous responses to the assistive force were observed across patients. Alterations of **C** in selected synergies were noted in a small subset of patients (Fig. 8B).

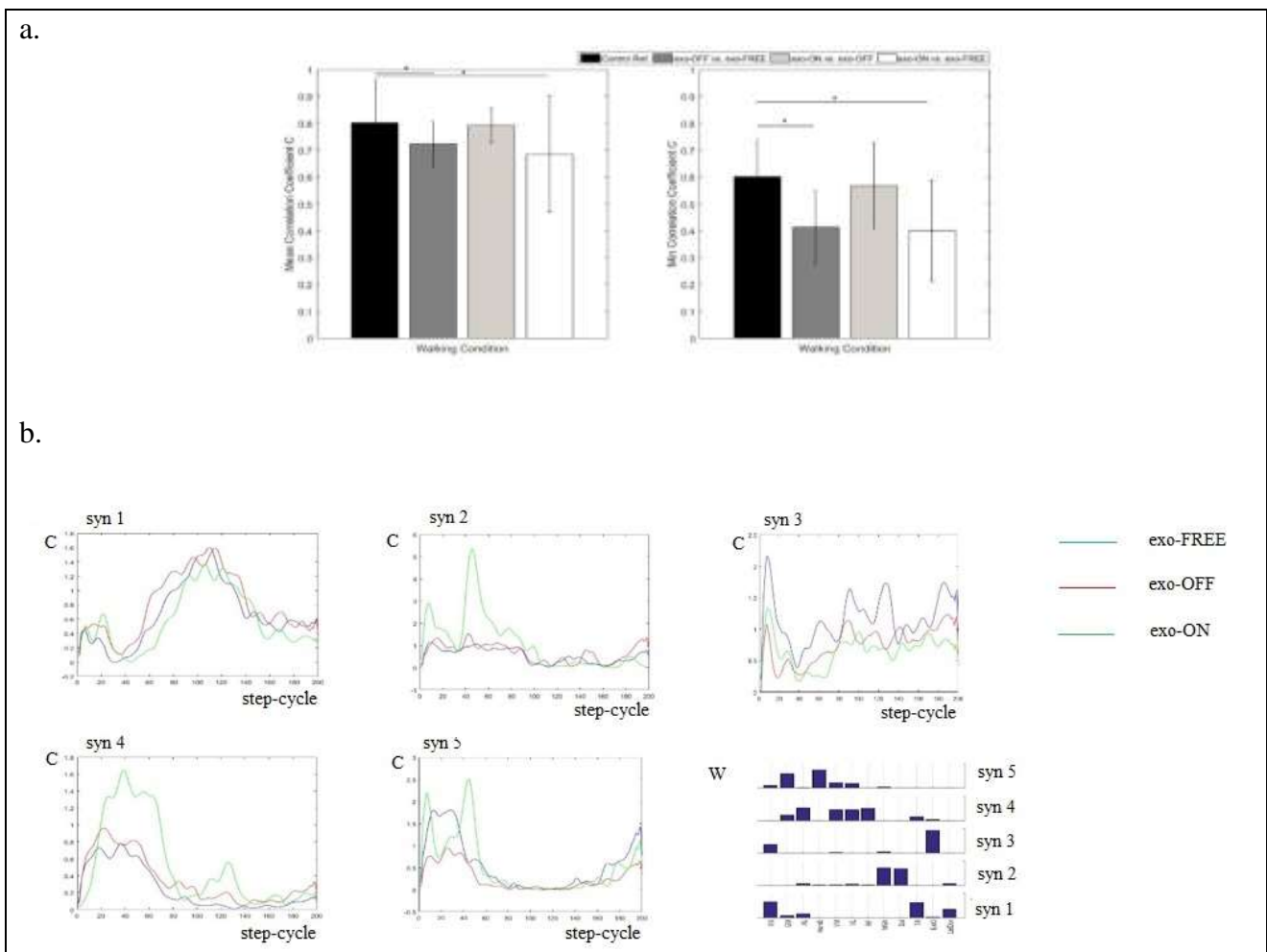


**Fig. 8. Correlation Levels between the Synergy Coefficient of activation C across Walking Conditions.** Panel a. Inter-condition Pearson's Correlation Coefficient  $r$  between the Cs of paretic synergies associated with exo-FREE, exo-OFF and exo-ON step-cycles (mean  $r$  and min  $r$ /subject-set, expressed as average  $\pm$  SD of the 10 stroke survivors). The symbol \* indicates  $P < 0.05$ . Panel b. Graphical representation of the **C** profile (averaged across the 10 step-cycles) during exo-FREE (blue colour), exo-OFF (red colour) and exo-ON (green colour) of the 5 preserved synergies obtained for one specific subject. Changes in **C** profile induced by the activation of the assistive torque (exo-ON) were evident for synergies 2 (mainly composed by the gastro-soles complex), 4 (vastus group + tibialis anterior) and 5 (gluteus maximus and hamstrings).

***Adaptation to the exoskeletal perturbations increased the similarity in muscle synergies between the paretic and non-paretic legs.***

In the exo-FREE epoch, subject-specific disruptions of the paretic-side muscle synergies as compared with the non-paretic-side synergies were observed, consistent with data from previous studies (Clark et al. 2010, Cheung et al. 2012). Inter-limb asymmetry of muscle synergies in the exo-FREE epoch was indicated by a low average minimum SP of  $0.561 \pm 0.071$ .

We then proceeded to ask whether exoskeletal perturbations may increase or decrease this inter-limb synergy similarity. Overall, changes in the paretic-side **W** induced by the active exoskeleton resulted in an increase in the mean and minimum SP between the paretic-side **W** and the synergies of the non-paretic exo-FREE baseline. If we specifically consider the changes attributable just to the assistive torque by comparing the inter-limb similarity from exo-OFF to exo-ON, the increase of the mean SP across these two epochs was statistically significant (Fig. 9A;  $P = 0.011$ , paired t-test).

We proceeded to take a closer look at the inter-limb mean SP of each of the 10 stroke survivors (Fig. 10). By comparing the inter-limb mean SP across the 3 epochs, we observed that 6 of the 10 subjects showed an increase in inter-limb synergy similarity from exo-FREE to exo-ON. If we selectively consider just the effects exerted by the assistive torque of the ankle robot by focusing on the OFF-to-ON transition, we observed an increase in the inter-limb synergy similarity in 9 of the 10 participants. The level of similarity increase demonstrated by these 9 subjects spanned a wide range: 4 subjects showed a  $<5\%$  increase; 2 subjects, 6-15%; and 3 subjects,  $>15\%$  (17.09%, 18.36%, and 19.45%, respectively).

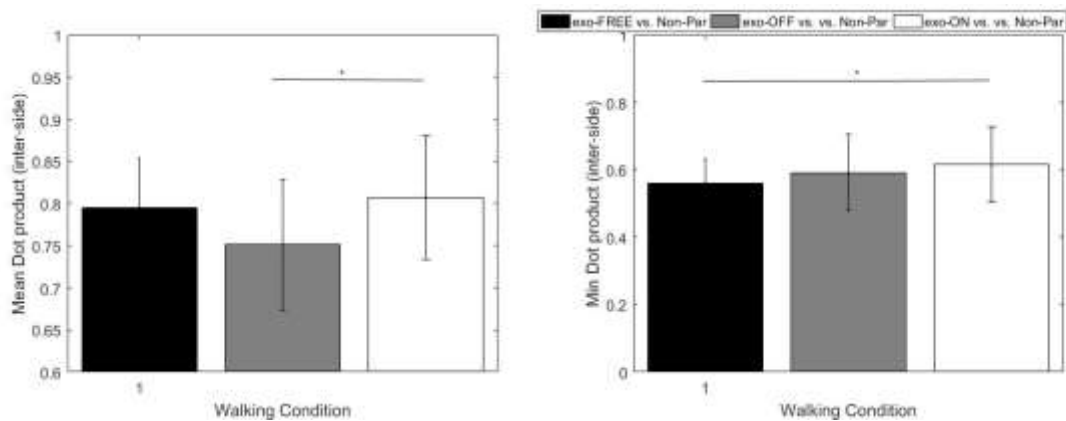


**Fig. 9. Inter-Side Comparison of Synergy Sets **W**.** Panel a. Inter-side mean SP (on the left) and min SP (on the right) (average  $\pm$  SD) obtained for exo-FREE, exo-OFF and exo-ON. Significant difference across walking condition ( $P < 0.05$ ) is highlighted by the asterisk \*.

***Across-epoch change in the inter-limb synergy similarity correlated with clinical scores.***

Given the wide range of across-epoch change in inter-limb synergy similarity across subjects, it is reasonable to ask whether this similarity depends on the status of the subjects, such as level of residual motor functions or degree of motor impairment as indicated by their clinical assessments. In exo-FREE vs. exo-ON, the change in inter-limb **W** similarity was not correlated ( $P > 0.05$ ) with the Berg Balance Scale (BBS), Lower-Extremities Fugl-Meyer sub-section scores (FMA-LE\*), or

with the Global Clinical Index (GCI) we defined based on the linear summation of the BBS and FMA-LE\* (Fig. 10C).

However, interesting correlations arose when we compared exo-OFF vs. exo-ON. A general positive trend emerged between the change in inter-limb **W** similarity and the GCI ( $r = +0.704$ ,  $P=0.023$ , Fig. 8C) and the BBS score ( $r = +0.683$ ,  $P=0.030$ , Fig. 10C), suggesting how residual motor and balance functions may influence the subjects' ability to respond to the exoskeleton within the training session.

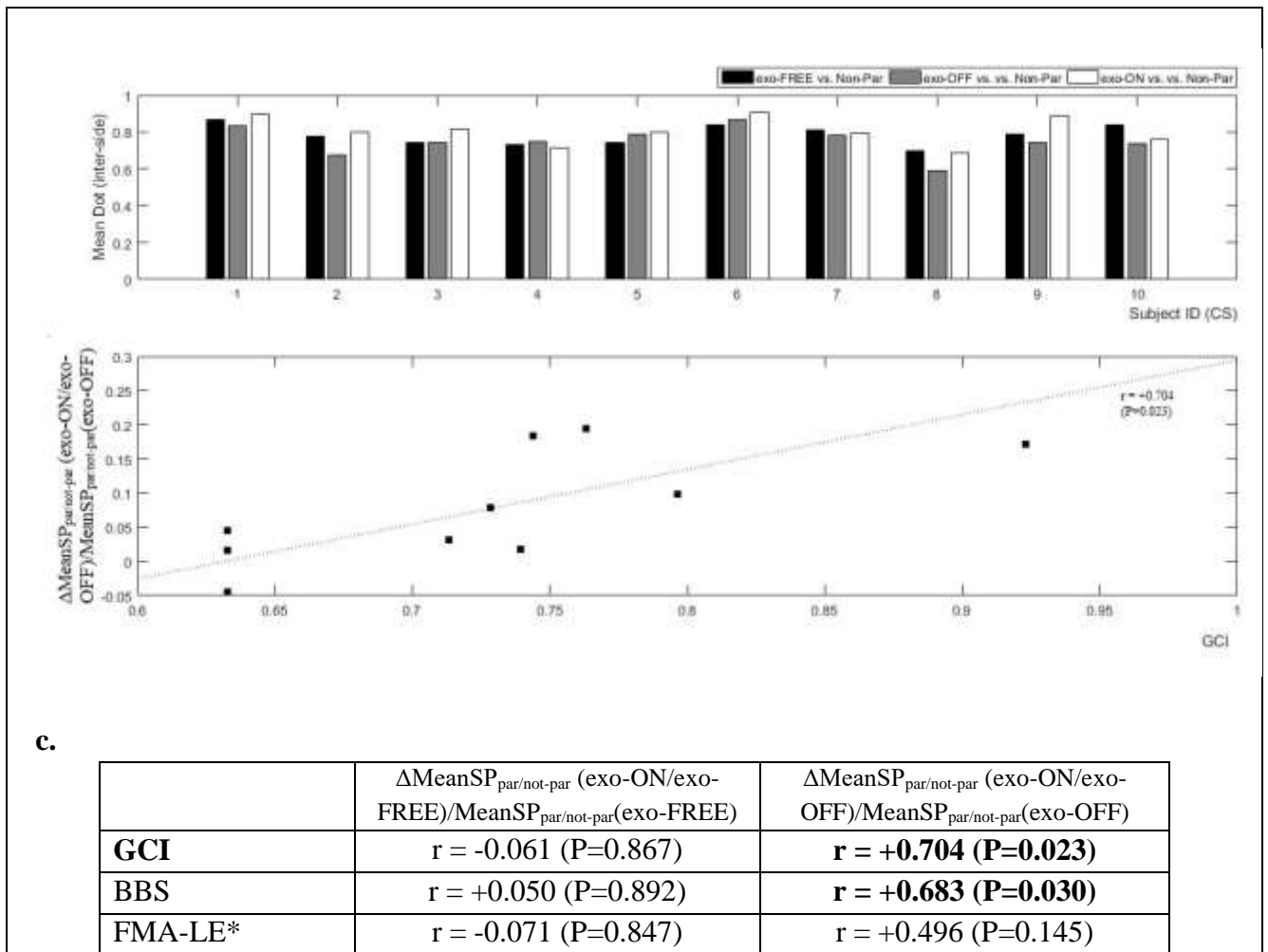


**Fig. 10. Correlation between the Changes in the Inter-Side Synergy Similarity and the Clinical Scores.** Panel a. Inter-Side (Paretic vs. Not-Paretic) mean  $\text{SP}_{\text{par/not-par}}$  and min  $\text{SP}_{\text{par/not-par}}$  across exo-FREE, exo-OFF and exo-ON condition, obtained for each of the 10 study participants. Panel b. Changes in inter-side similarity from exo-OFF to exo-ON, expressed as  $\Delta\text{MeanSP}_{\text{par/not-par}}(\text{exo-ON/exo-OFF})/\text{MeanSP}_{\text{par/not-par}}(\text{exo-OFF})$ , plotted in function of the GCI score. Panel c. Pearson's correlation coefficient ( $r$ ) and related P-value obtained between the changes in inter-side similarity and, respectively, BBS, FMA-LE\* and GCI scores.

## DISCUSSION

### **Gait training with powered exoskeleton for restoring muscle synergies in chronic survivors**

The most notable result obtained here is that even in chronic stroke survivors, forces from an ankle exoskeleton could elicit within-session changes in the synergies, in that the inter-side muscle-synergy similarity increased significantly from exo-FREE to exo-ON, and from exo-OFF to exo-ON. From the perspective of rehabilitation, the possibility of inducing synergy changes after stroke as a response to a perturbative force can be desirable. If this response involves selectively altering the abnormal synergies towards their normal patterns without compromising the other synergies unaffected by stroke, this exoskeletal training can be an intervention that drives neuroplasticity towards the direction of restoring the original, normal muscle patterns as the subject learns to adapt over multiple training sessions. This way, the resulting gait after training may be more naturalistic, and closer to being a true recovery from motor impairment (Cheung et al. 2012, Safavynia et al. 2011). Indeed, training with our ankle exoskeleton tested here may elicit such an ideal response of motor adaptation, at least for some stroke survivors. In 6 out of 10 subjects, the paretic-side synergies became more similar to the non-paretic-side reference synergies after they adapted to the exoskeletal assistive force (FREE-vs-ON comparison; Fig. 8A). It is conceivable that with sufficient training, the altered synergies adopted during training could be generalized to daily over-ground walking without exoskeleton.

In addition to our findings here, other recent studies have supported the possibility of a post-training increase in the similarity between impaired- and unimpaired-side muscle synergies in stroke survivors. In Ferrante et al. (2016) and Niu et al. (2018), a multi-muscle functional electrical stimulation (FES) intervention based on the normal muscle synergies induced alterations of the impaired-side synergies towards the normal patterns. Notably, such post-FES improvement in muscle synergy correlated positively with improvements of clinical, balance, and kinematic parameters. Here, we demonstrated that it is possible to elicit, in some chronic survivors, the emergence of more normal synergies even with training based on external assistive forces. It is possible that in both our study and the above-mentioned FES trials, as a result of the intervention, the voluntary motor task being trained for can be performed with closer-to-normal trajectories; the normalized sensory signals associated with the correct trajectories may then facilitate the expression of the normal synergies during task performance (Cheung et al. 2019, Lan et al. 2019). This mechanism is sensible, given that the spinal premotor interneurons that encode the synergies are innervated by proprioceptive afferent synapses (Levine et al. 2014), and that proprioceptive signals influence the choice of the specific synergies recruited for a behaviour (Kargo et al. 2009). In addition, since motor adaptation to perturbation likely involves the supraspinal regions such as the subthalamic and midbrain locomotor regions and the cerebellum (Takakusaki 2017), the alterations of synergies we observed may also be mediated by descending signals from the above higher motor centres.

In our data, we noted an increase in the number of muscle synergies from 5 to 6 from exo-OFF to exo-ON on the paretic legs of 2 subjects. As we have shown, this dimensionality increase is likely related to the uncoupling (or unmerging) of the synergies that were merged after the stroke event of those subjects (Clark et al. 2010, Cheung et al. 2012) (Fig. 7B, 7C), and is therefore a reflection of

the paretic-side synergies becoming closer to the normal synergies overall. Interestingly, the unmerging of synergies entailed individuated control of TA, a dorsiflexor involved in post-stroke foot drop, as well as EO, a trunk muscle important for balance control. Such unmerging is thus potentially important in any post-training improvement in both mobility and activities of daily living.

In contrast with our findings from chronic stroke survivors, previous works conducted on healthy individuals indicated that during walking, the presence of an exoskeleton does not alter the lower-limb muscle synergies (Gizzi et al. 2012, Jacobs et al. 2018). It is not impossible that the synergies of healthy subjects are less susceptible to being changed by perturbations because their intact sensorimotor system can allow more flexible recruitment of the existing synergies to counteract the external forces. But we note here that in those studies, healthy subjects performed gait training on a treadmill while our experimental protocol was based on over-ground walking. A direct translation of results from treadmill to over-ground gait demands caution. Ochoa et al. (2017) showed that human gait with an exoskeletal ankle robot differed between treadmill and over-ground walking. Importantly, neural adaptation of locomotor control appears to be more evident during over-ground training than treadmill training.

### **Heterogeneous responses to the exoskeletal assistive torque across stroke survivors**

As explained above, when the exoskeleton generates assistive torque in exo-ON, the external force may trigger alterations in the afferent signals sent to the CNS (Cheung et al. 2009 II), especially those arising from around the plantar sole and ankle joint. It is important to note that the lack of statistical significance for the change of the paretic-side muscle synergies from exo-OFF to exo-ON does not imply a total absence of change of synergy patterns across subjects. In fact, there was considerable heterogeneity among stroke survivors in their responses to the assistive torque. When examining the synergy minimum SPs for the OFF-to-ON paretic-side synergy change, we noticed that only half of the participants modified their synergies in the presence of the assistive torque; the remaining subjects showed a very high similarity between exo-OFF and exo-ON synergies (with minimum SP >0.79; Fig. 5B). For the same OFF-to-ON transition, across subjects the change in inter-side synergy similarity ranged from -4.4 to 19.4%, with 5 cases showing an increase of >7%. The above analysis suggests that not all patients were able to, or perhaps needed to, change their muscle synergies to adapt to the altered mechanical demands imposed by the device's assistive torque.

Our observation of heterogeneous responses is in line with the diversity of the subjects in our cohort. All participants were local community-dwelling volunteers with stroke onset dated >1 year before the experiment session. The location and extent of damage to the sensorimotor system in this cohort were almost certainly very diverse, which must have influenced their ability to adapt to external mechanical perturbations. Our result agrees with many prior studies (e.g., Semrau et al. 2015) that reported heterogeneous rehabilitation outcomes in clinical trials involving chronic stroke survivors.

The heterogeneity in response notwithstanding, our within-side comparisons did show that the most notable changes in the synergies from exo-OFF to exo-ON (SP < 0.70) involved activity components of the hamstrings, tibialis anterior (TA), and the gastrocnemius-soleus complex. The

involvement of the hamstrings may be explained by their prominent role in weight support and balance maintenance during walking. Alterations in TA may be related to its dorsi-flexor function during walking – a biomechanical function that was also implemented by the powered exoskeleton itself. The alteration of control signals sent to the gastrocnemius-soleus complex seen in 1 of the 10 recruited patients (Fig. 6C) may instead be explained by considering its role as an antagonist of TA. The increased dorsi-flexion introduced by the ankle robot might have triggered an altered response of the plantar-flexors with the purpose of decelerating the tibia segment prior to heel strike in order to avoid falling (Shiavi 1985).

### **Response to the exoskeletal assistive torque depends on residual motor and balance functions**

Interestingly, the heterogeneous responses to the exoskeletal assistive torque observed in our inter-side synergy analysis appeared to depend on the subjects' motor functional status at the time of training. Subjects with higher residual motor and balance functions, as indicated by our GCI clinical index, seemed to show more increase in inter-side synergy similarity from exo-OFF to exo-ON (Fig. 8B). Multiple previous works have documented correlations between levels of post-stroke motor impairment with the similarity of the stroke-affected-side synergies to the normative (Cheung et al. 2012, Ning et al. 2016, Cheung et al. 2019, Clark et al. 2010), and it has been proposed that muscle synergy may serve as a neurologically based marker of post-stroke impairment. It is thus reasonable to infer that the subjects who showed more within-session OFF-to-ON increase in inter-side synergy similarity would be more responsive to the training, perhaps more likely to achieve recovery from impairment by restoring the pre-stroke muscle commands.

We speculate that this dependency of the response on the residual motor function may partly originate from the specific design and function of the exoskeleton. As a unilateral device designed to be fixed along the shank of the impaired side, and with no other component for aiding balance support, the robot inevitably requires sufficient residual balance ability – as indicated by the BBS score – to sustain its perturbative forces so that the subject could at least walk with the device. At the same time, the subject would also need sufficient ankle flexion and extension abilities – as indicated by the FMA-LE\* score – to benefit from its assistive torque for foot dorsi- and plantar-flexion during training.

From a neural perspective, our result further underscores the crucial role of the surviving sensorimotor system in determining the subject's response to gait training. Better residual motor function, as indicated by a higher GCI, likely arises from a sensorimotor system that is less damaged by stroke. In subjects with higher GCI scores, the device's assistive torque can then more easily work with motor commands from the surviving sensorimotor system to elicit the sensory feedback signals needed to trigger adaptive motor outputs that are generated by closer-to-normal muscle synergies.

However, further studies involving more number and diversity of stroke survivors should be performed to probe more precisely how pre-therapy motor function and other factors (such as post-stroke duration, or the anatomy of the stroke lesions) may predict the magnitude of functional gain following training with our exoskeleton. In particular, changes in muscle synergy patterns should also be monitored during subsequent training sessions. We could not exclude *a priori* the possibility

that improvement in muscle synergy acquired in the initial sessions might not carry over to other sessions of the intervention.

### **The inactive exoskeleton as a significant perturbation that demands adaptation**

In this study, we also explored the effects induced on the muscle synergies by two kinds of perturbation introduced by the exoskeleton. Major synergy changes were found even when subjects walked wearing the inactive device (exo-OFF), but subsequent activation of the ankle robot from exo-OFF to exo-ON introduced, on average, relatively less degree of changes in both the synergies and their activations. Our results suggest that the device's weight and other afferent (e.g., cutaneous) stimulations resulting from the wearing of the exoskeleton may represent a very significant perturbation – certainly no less than the robot's assistive torque – that demands adaptation. The inactive device inevitably introduces a one-sided increase in the inertial load on the paretic side; but with a lower percentage of muscle mass and higher percentage of fat, the paretic limb of stroke survivors is, in most cases, weaker than the non-paretic limb. Immediate alterations in the body centre-of-mass position and muscle forces introduced in exo-OFF may trigger significant changes in the sensory feedback originating from the load receptors (Duysens et al. 2000). The resulting augmented, altered sensory feedback to the CNS may then induce adaptation through gradual changes in the feed-forward motor commands reflected as significant alterations of both the muscle synergies and their activation coefficients. Our interpretation here is in line with results of McGowan et al. (2010), who reported changes in the muscle-synergy profiles when alterations of mechanical demands were introduced during gait.

It remains possible that certain changes in the synergies and their coefficients elicited by the inactive exoskeleton are due to immediate, reactive adjustments of motor outputs triggered by the additional inertial load and cutaneous stimulations. Previous works in the frog and mouse have demonstrated that synergies organized in the spinal cord are accessible by cutaneous afferents (Kargo and Giszter, 2000; Levine et al. 2014). Also, inertial loading is known to cause immediate adjustments in the temporal activations of preserved muscle synergies (Cheung et al., 2009).

### **Conclusions**

The present work explores the application of muscle synergy analysis for the assessment of the neurological benefits associated with gait training using a robotic ankle exoskeleton. Our results suggest that as chronic stroke survivors walk with the exoskeleton, the resulting sensory inputs are sufficient to trigger recalibration of motor outputs within a single training session, so that the resulting muscle coordination patterns become more complex, and overall, more similar to the normal patterns on the non-paretic side. More importantly, our results hint at the possibility of driving neuroplasticity towards the direction of restoring the normal muscle patterns by imposing specific force perturbations to the paretic limb during training, thus demonstrating the potential of exoskeletal training to facilitate “true recovery” from motor impairment. It remains to be seen how the design of actuated exoskeleton can be further optimized to achieve even more of its therapeutic potential.

## REFERENCES

- Alia C, Spalletti C, Lai S, Panarese A, Lamola G, Bertolucci F, Vallone F, Di Garbo A, Chisari C, Micera S, Caleo M (2017): Neuroplastic Changes Following Brain Ischemia and their Contribution to Stroke Recovery: Novel Approaches in Neurorehabilitation. *Front Cell Neurosci.* 11: 76.
- Allen JL, Kautz SA, Neptune RR (2013): The influence of merged muscle excitation modules on poststroke hemiparetic walking performance. *Clin Biomech (Bristol, Avon)*; 28(6): 697-704.
- Berg K, Wood-Dauphinee S, Williams JI, Maki B (1992): Measuring balance in the elderly: validation of an instrument. *Can J Pub, 83 (Suppl. 2), S7-S11.*
- Bortole M, Venkatakrishnan A, Zhu F, Moreno JC, Francisco GE, Pons JL, Contreras-Vidal JL (2015): The H2 robotic exoskeleton for gait rehabilitation after stroke: early findings from a clinical study. *Journal of NeuroEngineering and Rehabilitation*, 12:54.
- Cheung VCK, Bizzi E, 2013: The Neural Origin of Muscle Synergies. *Front Comput Neurosci* Apr 29;7:51.
- Cheung VCK, D'Avella A, Tresch MC, Bizzi E (2005): Central and Sensory Contributions to the Activation and Organization of Muscle Synergies during Natural Motor Behaviors. *Journal of Neuroscience*, 25(27): 6419-6434.
- Cheung VCK, Niu CM, Li S, Xie Q, Lan N (2019): A Novel FES Strategy for Post-Stroke Rehabilitation Based on the Natural Organization of Neuromuscular Control. *IEEE Rev Biomed Eng.* 12: 154-167.
- Cheung VCK, Piron L, Agostini M, Silvoni S, Turolla A, Bizzi E (2009), I: Stability of muscle synergies for voluntary actions after cortical stroke in humans. *PNAS* 106(46): 19563–19568.
- Cheung VCK, d'Avella A, Bizzi E (2009), II: Adjustments of motor pattern for load compensation via modulated activations of muscle synergies during natural behaviors. *Journal of neurophysiology* 101 (3), 1235-1257.
- Cheung VCK, Turolla A, Agostini M, Silvoni S, Bennis C, Kasi P, Paganoni S, Bonato P, Bizzi E (2012): Muscle synergy patterns as physiological markers of motor cortical damage. *PNAS* 109(36): 14652–14656.
- Chia N, Ambrosini E, Baccinelli W, Nardone A, Monticone M, Ferrigno G, Pedrocchi A, Ferrante S (2015): A multi-channel biomimetic neuroprosthesis to support treadmill gait training in stroke patients. *Conf Proc IEEE Eng Med Biol Soc.:* 7159-62.
- Clark DJ, Ting LH, Zajac FE, Neptune RR, Kautz SA (2010): Merging of healthy motor modules predicts reduced locomotor performance and muscle coordination complexity post-stroke. *J Neurophysiol.* 103(2):844-857.
- Coscia M, Cheung VCK, Tropea P, Koenig A, Monaco V, Bennis C, Micera S, Bonato P (2014): The effect of arm weight support on upper limb muscle synergies during reaching movements. *J Neuroeng Rehabil.*, 11:22. doi: 10.1186/1743-0003-11-22.
- Delp SL, Anderson FC, Arnold AS, Loan P, Habib A, John CT, Guendelman E, Thelen DG (2007): OpenSim: Open-source Software to Create and Analyze Dynamic Simulations of Movement. *IEEE Trans Biomed Eng.*, 54(11): 1940-50.
- Dickstein R (2008): Rehabilitation of Gait Speed After Stroke: A Critical Review of Intervention Approaches. *Neurorehabil Neural Repair.*, 22(6): 649-60.
- Duysens J, Clarac F, Cruse H (2000): Load-Regulating Mechanisms in Gait and Posture: Comparative Aspects. *Physiological Reviews*, 80(1):83-133.
- Ferrante S, Bejarano NC, Ambrosini E, Nardone A, Turcato AM, Monticone M, Ferrigno G, Pedrocchi A (2016): A Personalized Multi-Channel FES Controller Based on Muscle Synergies to Support Gait Rehabilitation after Stroke. *Front. Neurosci.*, 16 September 2016
- Fugl-Meyer AR, Jaasko L, Leyman I (1975): The post stroke hemiplegic patient. I. A method for evaluation of physical performance. *Scandinavian Journal of Rehabilitation Medicine*, 7(1): 13-31. Gizzi L, Feldbæk Nielsen J, Felici F, Ivanenko YP, Farina D (2011): Impulses of activation but not motor modules are preserved in the locomotion of subacute stroke patients. *J Neurophysiol*, 106: 202–210.
- Gizzi L, Nielsen JF, Felici F, Moreno JC, Pons JL, Farina D (2012): Motor modules in robot-aided walking. *J Neuroeng Rehabil.* 9:76.
- Hashiguchi Y, Ohata K, Kitatani R, Yamakami N, Sakuma K, Osako S, Aga Y, Watanabe A, Yamada S (2016): Merging and Fractionation of Muscle Synergy Indicate the Recovery Process in Patients with Hemiplegia: The First Study of Patients after Subacute Stroke. *Hindawi Publishing Corporation Neural Plasticity*, Article ID 5282957.
- Hermens HJ, Freriks B, Disselhorst-Klug C, Rau G (2000): Development of recommendations for SEMG sensors and sensor placement procedures. *Journal of Electromyography and Kinesiology*, 10(5):361-374.

- Hesse S, Tomelleri C, Bardeleben A, Werner C, Waldner A (2012): Robot-assisted practice of gait and stair climbing in nonambulatory stroke patients. *J Rehabil Res Dev*; 49(4): 613-22 (ISSN: 1938-1352).
- Houldin A, Luttin K, Lam T (2011): Locomotor adaptations and aftereffects to resistance during walking in individuals with spinal cord injury. *J Neurophysiol* 106: 247–258.
- Husemann B, Muller F, Krewer C, Heller S, Koenig E (2007): Effects of locomotion training with assistance of a robot-driven gait orthosis in hemiparetic patients after stroke: a randomized controlled pilot study. *Stroke*, 38(2): 349-354.
- Jacobs DA, Koller JR, Steele KM, Ferris DP (2018): Motor modules during adaptation to walking in a powered ankle exoskeleton. *Journal of NeuroEngineering and Rehabilitation*, 15(1): 2.
- Kargo WJ and Giszter SF (2000): Rapid Correction of Aimed Movements by Summation of Force-Field Primitives. *Journal of Neuroscience*, 20 (1) 409-426.
- Kargo, W. J., Ramakrishnan, A., Hart, C. B., Rome, L. C., & Giszter, S. F. (2009). A simple experimentally based model using proprioceptive regulation of motor primitives captures adjusted trajectory formation in spinal frogs. *Journal of neurophysiology*, 103(1), 573-590.
- Kasai R, Takeda S (2016): The effect of a hybrid assistive limb® on sit-to-stand and standing patterns of stroke patients, *J. Phys. Ther. Sci*: 1786-1790.
- Takakusaki K (2017): Functional Neuroanatomy for Posture and Gait Control. *J Mov Disord*. 10(1): 1–17.
- Kibushi B, Hagio S, Moritani T, Kouzaki M (2018): Speed-Dependent Modulation of Muscle Activity Based on Muscle Synergies during Treadmill Walking. *Front. Hum. Neurosci*. 12:4.
- Lamola G, Fanciullacci C, Rossi B, Chisari C (2014): Clinical evidences of brain plasticity in stroke patients. *Archives Italiennes de Biologie*, 152: 259-271.
- Lan N, Cheung VCK, Gandevia SC (2016): Editorial: Neural and Computational Modeling of Movement Control. *Front. Comput. Neurosci*, 31 August 2016
- Lan N, Niu CM, Hao M, Chou C-H, Dai C (2019): Achieving Neural Compatibility With Human Sensorimotor Control in Prosthetic and Therapeutic Devices. *Medical Robotics and Bionics IEEE Transactions* 1,3: 122-134.
- Lee DD, Seung HS (1999): Learning the parts of objects by non-negative matrix factorization. *Nature* 401: 788-791.
- Levine AJ, Hinckley CA, Hilde KL, Driscoll SP, Poon TH, Montgomery JM, et al. (2014): Identification of a cellular node for motor control pathways. *Nat. Neurosci*. 17, 586–593.
- Louie, D. R., & Eng, J. J. (2016). Powered robotic exoskeletons in post-stroke rehabilitation of gait: a scoping review. *Journal of neuroengineering and rehabilitation*, 13(1), 53.
- Mbourou, GA, Lajoie Y, Teasdale N (2003): Step length variability at gait initiation in elderly fallers and non-fallers, and young adults. *Gerontology* 49, 21-26.
- McGowan CP, Neptune RR, Clark DJ, Kautz SA (2010): Modular control of human walking: Adaptations to altered mechanical demands. *J Biomech*. 43(3): 412.
- Mehta S, Pereira S, Viana R, Mays R, McIntyre A, Janzen S, Teasell RW (2012): Resistance training for gait speed and total distance walked during the chronic stage of stroke: a meta-analysis. *Top Stroke Rehabil*. 19(6): 471-8.
- Meyer AJ, Eskinazi I, Jackson JN, Rao AV, Patten C, Fregly BJ (2016): Muscle synergies Facilitate Computational Prediction of subject-specific Walking Motions. *Frontiers in Bioengineering and Biotechnology*, 13(4), 77.
- Miljkovi N, Milovanovi I, Draginc A, Konstantinovi L, Popovi DB (2013): Muscle synergies with Walkaround® postural support vs. “cane/therapist” assistance. *NeuroRehabilitation*, 33: 491-501.
- Mukaka MM (2012): Statistics Corner: A guide to appropriate use of Correlation coefficient in medical research. *Malawi Medical Journal*, 24(3): 69-71.
- Murray SA, Ha KH, Hartigan C, Goldfarb M (2015): An Assistive Control Approach for a Lower-Limb Exoskeleton to Facilitate Recovery of Walking Following Stroke. *IEEE Transactions On Neural Systems And Rehabilitation Engineering*, 3: 441-449.
- Nishida K, Hagio S, KibushiB, MoritaniT, Kouzaki M (2017): Comparison of muscle synergies for running between different foot strike patterns. *PLoS ONE* 12(2):e0171535.
- Niu, C. M., Bao, Y., Zhuang, C., Li, S., Wang, T., Cui, L., Xie, Q., Lan, N. (2019). Synergy-based FES for post-stroke rehabilitation of upper-limb motor functions. *IEEE Transactions on Neural Systems and Rehabilitation Engineering*, 27(2), 256-264.

- Nurse MA & Nigg BM (2001): The effect of changes in foot sensation on plantar pressure and muscle activity. *Clinical Biomechanics*, 16(9): 719–727.
- Pennycott A, Wyss, Vallery H, Klamroth-Marganska V, Riener R (2012): Towards more effective robotic gait training for stroke rehabilitation: a review. *Journal of NeuroEngineering and Rehabilitation*; 9:65.
- Polese JC, Ada L, Dean CM, Nascimento LR, Teixeira-Salmela LF (2013): Treadmill training is effective for ambulatory adults with stroke: a systematic review. *J Physiother.* 59: 73-80.
- Pons JL (2019) Witnessing a wearable transition. *Science*, 365(6454): 636-637.
- Safavynia SA, Torres-Oviedo G, Ting LH (2011): Muscle Synergies: Implications for Clinical Evaluation and Rehabilitation of Movement. *Top Spinal Cord Inj Rehabil*; 17(1): 16-24.
- Schiavi R, Frigo C, Pedotti A (1998): Electromyographic signals during gait: criteria for envelope filtering and number of strides. *Med. Biol. Eng. Comput.* 35: 171-178.
- Semrau JA, Herter TM, Scott SH, Dukelow SP (2015): Examining Differences in Patterns of Sensory and Motor Recovery After Stroke With Robotics. *Stroke* 46: 3459-3469.
- Shiavi R (1985): Electromyographic patterns in adult locomotion: a comprehensive review. *Journal of Rehabilitation Research and Development*, 22(3), 85–98.
- Shumway-Cook A and Woollacott MH (2002): *Motor Control: Theory and Practical Applications* (2nd ed.). Lippincott Williams & Wilkins.
- Steele KM, Jackson RW, Shuman BR, Collins SH (2017): Muscle recruitment and coordination with an ankle exoskeleton. *Journal of Biomechanics* 59: 50–58.
- Sylos-Labini F, La Scaleia V, d'Avella A, Pisotta I, Tamburella F, Scivoletto G, Molinari M, Wang S, Wang L, van Asseldonk E, van der Kooij H, Hoellinger T, Cheron G, Thorsteinsson F, Ilzkovitz M, Gancet J, Hauffe R, Zanov F, Lacquaniti F, Ivanenko YP (2014): EMG patterns during assisted walking in the exoskeleton. *Front Hum Neurosci.* 8: 423.
- Takei, T., Confais, J., Tomatsu, S., Oya, T., & Seki, K. (2017). Neural basis for hand muscle synergies in the primate spinal cord. *Proceedings of the National Academy of Sciences*, 114(32), 8643-8648.
- Tan CK, Kadone H, Watanabe H, Marushima A, Yamazaki M, Sankai Y, Suzuki K (2018): Lateral Symmetry of Synergies in Lower Limb Muscles of Acute Post-stroke Patients After Robotic Intervention. *Front Neurosci.* 12: 276.
- Teasell RW, Murie Fernandez M, McIntyre A, Mehta S (2014): Rethinking the continuum of stroke rehabilitation. *Arch Phys Med Rehabil.* 95(4): 595-6.
- Tong RK, Ng MF, Li LS, (2006): Effectiveness of Gait Training Using an Electromechanical Gait Trainer, With and Without Functional Electric Stimulation, in Subacute Stroke: A Randomized Controlled Trial. *Archives of Physical Medicine and Rehabilitation*, 87(10): 1298-1304.
- Winstein CJ, Stein J, Arena R et al. (2016): Guidelines for Adult Stroke Rehabilitation and Recovery. A Guideline for Healthcare Professionals From the American Heart Association/American Stroke Association. *Stroke*, 47: 000-000.
- Yeung LF, Ockenfeld C, Pang MK, Wai HW, Soo OY, Li SW, Tong KY (2017): Design of an Exoskeleton Ankle Robot for Robot-Assisted Gait Training of Stroke Patients. 2017 International Conference on Rehabilitation Robotics (ICORR) QEII Centre, London, UK.
- Yokoyama H, Ogawa T, Kawashima N, Shinya M, Nakazawa K (2016): Distinct sets of locomotor modules control the speed and modes of human locomotion. *Sci Rep.*, 6: 36275.

**SUPPLEMENTARY MATERIAL**

**Table S1.** Details of the sub-sessions of the Fugl-Meyer Assessment (FMA) considered in our experimental protocol (Fugl-Meyer et al. 1975).

<u>Sub-sections from E. Lower Extremity</u>				
<b>Volitional movement within synergies</b>	Supine position	none	partial	full
Flexor synergy	Hip flexion	0	1	2
	Knee flexion	0	1	2
	Ankle dorsiflexion	0	1	2
Extensor synergy	Hip extension	0	1	2
	Hip adduction	0	1	2
	Knee extension	0	1	2
	Ankle plantarflexion	0	1	2
<b>Volitional movement mixing synergies, sitting position, knee 10 cm from the edge of the chair/bed</b>				
Knee flexion from actively or passively extended knee	No active motion	0		
	Less than 90° active flexion, palpate tendons or hamstrings		1	
	Knee flexion beyond 90°, palpate tendons or hamstrings			2
Ankle dorsiflexion compare with unaffected side	No active motion	0		
	Limited dorsiflexion		1	
	Complete dorsiflexion			2
<b>Volitional movement with little or no synergy, standing position, hip at 0°</b>				
Knee flexion to 90°, hip at 0°, balance support is allowed	No active motion/simultaneous hip flexion	0		
	Less than 90° knee flexion or hip flexion during movement		1	
	At least 90° knee flexion without simultaneous hip flexion			2
Ankle dorsiflexion, compare with unaffected side	No active motion	0		
	Limited dorsiflexion		1	
	Complete dorsiflexion			2
<u>Sub-sections from F. Coordination/Speed</u>				
Supine, after one trial with both legs, blind-folded, heel to knee cap of the opposite leg, 5 times as fast as possible				
		marked	slight	none
Tremor		0	1	2
Dysmetria	Pronounced or unsystematic	0		
	Slight and systematic		1	
	No dysmetria			2
Time	> 5 sec		2-5 sec	< 1 sec
	More than 5 seconds slower than unaffected side	0		
	2-5 seconds slower than unaffected side		1	
	Maximum difference of 1 second between sides			2
<b>TOTAL</b>				<b>Max = 30</b>